Performance Assessment of Run-to-Run Mixed Product Control Schemes for Overlay Lithography Processes

An-Chen Lee*
Department of Mechanical Engineering
National Chiao Tung University
Hsinchu City, Taiwan, R.O.C.
aclee@mail.nctu.edu.tw

Tzu-Wei Kuo
Department of Mechanical Engineering
National Chiao Tung University
Hsinchu City, Taiwan, R.O.C.
tzkuo@nctu.edu.tw

Wen-Thong Chang
Photonics and Communication Engineering
Asia University,
Wufeng, Taichung, Taiwan, R.O.C.
wtchang@asia.edu.tw

Abstract—**Advanced process control (APC) has been recognized as a proper tool for maximizing profitability of semiconductor manufacturing facilities by improving efficiency and product quality. Run-to-run (RtR) process control with good quality and reliable performance for APC applications are most applicable. This paper conducts performance assessment on four RtR mixed product control schemes which are available in the literature: thread EWMA (t-EWMA), thread PCC (t-PCC), JADE and m-dEWMA, with actual overlay historical mixed product processes data. Meantime, the comparison also includes the moving average three (MA(3)) method which is commonly used in semiconductor factories. The simulation results revealed that t-EWMA, t-PCC and m-dEWMA could be used in overlay mixed product processes, but the JADE was not recommended to be applied in overlay mixed product processes.**

Keywords- advanced process control; run-to-run; overlay; mixed product; m-dEWMA control scheme;

I. INTRODUCTION

In the last decade, the run-to-run (RtR) control has been used or proposed for common and critical semiconductor manufacturing processes such as chemical-mechanical planarization (CMP) and lithography line width control [1]. The EWMA and d-EWMA controllers are commonly used by engineers in semiconductor manufacturing, and the control performance and the stability of these two controllers have been studied widely by several authors [2-4].

The RtR overlay lithography process control issue also has been investigated by some authors. Lin [5] utilized multiple linear regression method to analyze the overlay accuracy model and study the feasibility of using linear methods to solve parameters of nonlinear overlay equations. Martinez [6] combined EWMA controller and recursive least squares (RLS) method to estimate the overlay tool bias in overlay process. The simulation results show that their controller reduced the rework rate with 30% in average. Bode [7] and Middlebrooks [8] utilized model predictive control (MPC) to deal with the disturbance caused by overlay processes. Based on the tool-product-layer specifically combination, the MPC had well ability to eliminate the disturbance caused by overlay processes.

Recently, Lee [9] presented a unified framework called the output disturbance observer (ODOB) structure for the EWMA controller, the d-EWMA controller and the predictor corrector controller (PCC) controller. The work enhances insight into the well-known established algorithms, and contributes to better understanding of how these algorithms operate and why they can be used successfully in practical application. Other methods in RtR controllers have also been proposed and applied in semiconductor manufacturing [10-12].

However, the above papers did not consider the processes in mixed product situation. Only a few studies have addressed the RtR control of a mixed product process plant, such as: Just-in-time Adaptive Disturbance Estimation (JADE) [13], tool-based and product-based EWMA control (PB-EWMA or t-EWMA) [14], threaded PCC (t-PCC) [15], CF-EWMA [16] and m-dEWMA [17] controllers. Expect the m-dEWMA control scheme has been proven the control capacity in actual CMP mixed product process [17], the others are only verified their control performance with numerical simulations.

In this paper, one will compare the control performance of t-EWMA, t-PCC, JADE and m-dEWMA with actual overlay mixed product processes data. Besides, one will utilize the moving average 3 (MA(3)) control method which is widely used in overlay mixed product processes in comparison with these four mixed product control schemes. In section Ⅱ, one will briefly introduce the application of m-dEWMA control scheme in overlay mixed product process. The characteristic of overlay process, the control simulation and the discussion are

addressed in section Ⅲ. Finally, the conclusions are drawn in the section Ⅳ.

II. PROBLEM DESCRIPTION

Consider historical data of the mixed product overlay process as shown in Fig. 1, where the X-axis represents lot number (run) and the Y-axis represents the disturbance of the product and layer's combination. The historical data contains one tool, two products and two layers, and there are four manufacturing threads in this production situation. Fig. 1

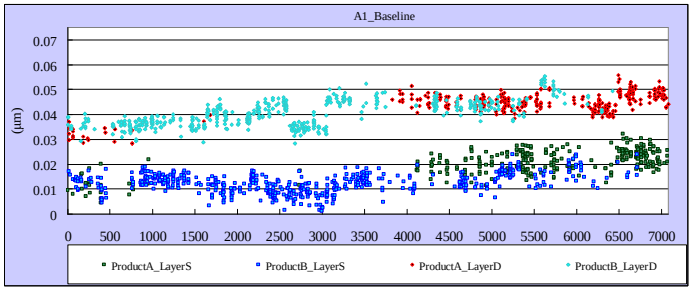

Figure 1. Historical data of specify products and layers

presents that the characteristic drift in the overlay disturbance is caused by tool over the long term, and each manufacturing thread has its individual initial intercept.

According to characteristic of overlay processes as mention above, this paper proposes a modified double EWMA (m-dEWMA) control with break-product compensation for the drift disturbance caused by the tool. Considering the one tool and multi-products processes, the process model can be presented as:

$$y_{i,k} = \alpha_i + \beta_i u_{i,k} + \delta_{i,k} \tag{1}$$

where $y_{i,k}$ denotes process output, α_i denotes the initial intercept of product i, $u_{i,k}$ denotes the control recipe of product i, β_i denotes actual process gain for product i, $\delta_{i,k}$ denotes process disturbance, k denotes the run numbers. The following cases demonstrate the m-dEWMA updating procedure:

Case 1. For the first run of product i

$$\hat{d}_{i,k} = \lambda_{1,i}\left(y_{i,k} - b_i u_{i,k}\right) + \left(1-\lambda_{1,i}\right)\left(\hat{d}_{i,0} + \hat{p}_{k-1}\right) \tag{2}$$

$$\hat{p}_k = \lambda_2\left(y_{i,k} - b_i u_{i,k} - \hat{d}_{i,0}\right) + \left(1-\lambda_2\right)\hat{p}_{k-1} \tag{3}$$

Case 2. For product i keeping on processing

$$\hat{d}_{i,k} = \lambda_{1,i}\left(y_{i,k} - b_i u_{i,k}\right) + \left(1-\lambda_{1,i}\right)\left(\hat{d}_{i,k-1} + \hat{p}_{k-1}\right) \tag{4}$$

$$\hat{p}_k = \lambda_2\left(y_{i,k} - b_i u_{i,k} - \hat{d}_{i,k-1}\right) + \left(1-\lambda_2\right)\hat{p}_{k-1} \tag{5}$$

Case 3. For break-product (product j)

$$\begin{aligned} \hat{d}_{j,k} &= \hat{d}_{j,k-1} + \hat{p}_{k-1} \\ &= \hat{d}_{j,k-2} + \hat{p}_{k-2} + \hat{p}_{k-1} \\ &\vdots \\ &= \hat{d}_{j,k-n} + \sum_{m=1}^{n} \hat{p}_{k-m} \end{aligned} \tag{6}$$

Case 4. For product change (product i changes into product j)

$$\begin{aligned} \hat{d}_{j,k} &= \lambda_{1,j}\left(y_{j,k} - b_j u_{j,k}\right) + \left(1-\lambda_{1,j}\right)\left(\hat{d}_{j,k-1} + \hat{p}_{k-1}\right) \\ &= \lambda_{1,j}\left(y_{j,k} - b_j u_{j,k}\right) + \left(1-\lambda_{1,j}\right)\left(\hat{d}_{j,k-n} + \sum_{m=1}^{n} \hat{p}_{k-m}\right) \end{aligned} \tag{7}$$

$$\begin{aligned} \hat{p}_k &= \lambda_2\left(y_{j,k} - b_j u_{j,k} - \hat{d}_{j,k-1}\right) + \left(1-\lambda_2\right)\hat{p}_{k-1} \\ &= \lambda_2\left(y_{j,k} - b_j u_{j,k} - \hat{d}_{j,k-n} - \sum_{m=1}^{n-1} \hat{p}_{k-m}\right) + \left(1-\lambda_2\right)\hat{p}_{k-1} \end{aligned} \tag{8}$$

Case 1 shows the update procedure at the first run of product i ($i = 1, 2, 3...$), where $\hat{d}_{i,0}$ and $\hat{p}_{k-1}$ denote the initial intercept estimation for product i and the drift estimate for tool at run k-1, respectively. The b_i denotes the model gain, $\lambda_{1,i}$ and λ_2 denote the weights of m-dEWMA control scheme. When product i keeps on processing (Case 2), the intercept and drift estimations are updated by (4)-(5), where $\hat{d}_{i,k}$ is the intercept estimation of product i on run k, $\hat{p}_k$ is the drift estimation. Meanwhile, the intercept estimations of break product j, $\hat{d}_{j,k}$, is updated by the drift estimation , $\hat{p}_{k-1}$, of product i on run k-1 (Case 3). In other words, product i and product j share the drift estimation because the drift disturbance is caused by the tool. In the Case 4, the first run of product j will utilize the previous estimations on run k-n by assuming product i has been processed for n-1 runs (6) and current measured data to update the intercept and drift estimations. The next run (k+1) control input of product i can be calculated by:

$$u_{i,k+1} = \frac{T_i - \left(\hat{d}_{i,k} + \hat{p}_k\right)}{b_i} \tag{9}$$

where T_i is process target of product *i*.

III. LITHOGRAPHY OVERLAY MIXED PRODUCT PROCESS

A. Background

Lithography overlay process is the critical process in semiconductor manufacturing. The control of overlay tolerance is one of the key design problems of the manufacturing of integrated circuits. By definition, overlay is the displacement error of an exposed image field relative to the previous exposed image field [5]. There are a number of causes leading to overlay errors, including system environment, stepper, mask accuracy, change in line width, and lens distortion [18]. Lin and Wu proposed an overlay accuracy model [5] which combined intrafield (field term) [19] and interfiled (wafer term) [20] overlay error models as follows:

$$\begin{aligned} dx(X,Y,x,y) &= E_{wx}(X,Y)+E_{fx}(x,y)+r_x(X,Y,x,y) \\ &= T_{wx}-R_{wx}Y+M_{wx}X+B_{wx}Y^2+T_{fx}-R_{fx}y+M_{fx}x-T_{xx}x^2 \\ &\quad -T_{yx}xy+W_{fx}y^2+D_{3x}x\left(x^2+y^2\right)+D_{5x}x\left(x^2+y^2\right)^2 \\ &\quad +D_{7x}x\left(x^2+y^2\right)^3+r_x \end{aligned} \tag{10}$$

$$\begin{aligned} dy(X,Y,x,y) &= E_{wy}(X,Y)+E_{fy}(x,y)+r_y(X,Y,x,y) \\ &= T_{wy}-R_{wy}Y+M_{wy}Y+B_{wy}X^2+T_{fy}-R_{fy}x \\ &\quad +M_{fy}y-T_{yy}y^2-T_{xy}xy+W_{fy}x^2+D_{3y}y\left(x^2+y^2\right) \\ &\quad +D_{5y}y\left(x^2+y^2\right)^2+D_{7y}y\left(x^2+y^2\right)^3+r_y \end{aligned} \tag{11}$$

where (x,y) denotes the sample location in the field coordinate system; E_{fx} and E_{fy} denote the error from the intrafield sources, T_{fx} and T_{fy} both constant parameters, denote the horizontal translation of the exposure field image in the X-axis and Y-axis directions; $R_{fx}y$ and $R_{fy}x$ denote the rotation angle of the exposure field image; M_{fx} and M_{fy} are image magnification parameters; T_{xx}, T_{xy}, T_{yx} and T_{yy} denote the trapezoid parameters of mask; W_{fx} and W_{fy} denote the wedge distortion parameters or tilting of the lens elements; D_{3x}, D_{3y}, D_{5x}, D_{5y}, D_{7x} and D_{7y} denote the high-order distortion parameters of the filter lens, which belong to the rotational symmetrical lens design. (X,Y) denotes the location of field center in the wafer coordinate system. The positioning error source between the mask and wafer primarily come from the aligning error and the motion error of the mechanism of wafer movement. E_{wx} and E_{wy} denote the overlay cause by interfiled sources in the X-axis and Y-axis directions, respectively, where T_{wx} and T_{wy} denote the translation error of the X-axis and Y-axis aligned by the wafer; R_{wx} and R_{wy} denote the rotation error of the wafer; M_{wx} and M_{wy} denote the linear magnification parameters of the interferometer scaling; B_{wx} and B_{wy} denote the stage bow parameters which are primarily cause by block mirror imperfections. *dx* and *dy* denote the overlay measured in the X-axis and Y-axis directions, respectively, on the wafer, r_x and r_y denote the residual overlay.

In actual overlay manufacturing process, the trapezoid (W_{fx} and W_{fy}), wedge distortion (T_{xx}, T_{xy}, T_{yx} and T_{yy}), stage bow (B_{wx} and B_{wy}) and the high-order terms (D_{3x}, D_{3y}, D_{5x}, D_{5y} D_{7x} and D_{7y}) are difficult to regulate during processing wafers. Hence, the stepper/scanner equipment producer, Canon Inc., utilizes (10)-(11) and simplifies the model to monitor and control the overlay error during manufacturing products as shown follow:

$$d_{X+x} = T_{wX}+M_{wX}X-R_{wX}Y+M_{fx}x-R_{fx}y \tag{12}$$

$$d_{Y+y} = T_{wY}+M_{wY}Y+R_{wY}X+M_{fy}y+R_{fy}x \tag{13}$$

Equations (12) 錯誤！找不到參照來源。 and (13)錯誤! 找不到參照來源。 can be rewritten as:

$$d_{X+x} = A_1+A_3X-A_5Y+X_7x-X_8y \tag{14}$$

$$d_{Y+y} = A_2+A_4Y+B_5X+Y_7y+Y_8x \tag{15}$$

where $A_1 = T_{wX}$ the translation error of X-axis aligned by the wafer, $A_2 = T_{wY}$ the translation error of Y-axis aligned by the wafer, $A_3 = M_{wX}$ linear magnification of X-axis aligned by the wafer, $A_4 = M_{wY}$ linear magnification of Y-axis aligned by the wafer, $A_5 = R_{wX}$ rotation error of the wafer, $B_5 = R_{wY}$ rotation error of the wafer, $X_7 = M_{fx}$ image magnification of X-axis aligned by the field, $X_8 = R_{fx}$ rotation angle of the exposure field image, $Y_7 = M_{fy}$ image magnification of X-axis aligned by the field and $Y_8 = R_{fy}$ rotation angle of the exposure field image. Fig. 2 shows the overlay error pattern of (12)-(13).

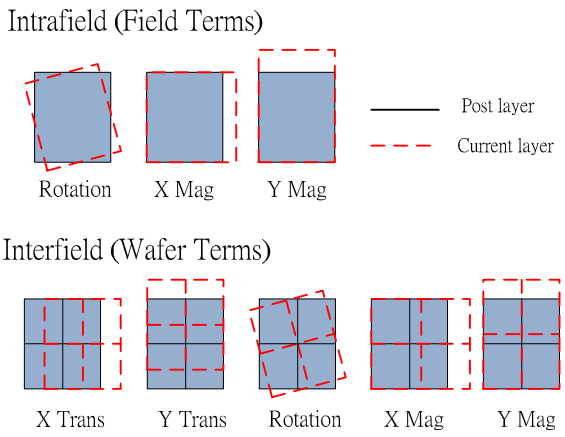

Figure 2. Overlay error pattern

B. *Simulation with Historical Data*

In order to compare the control capacity of m-dEWMA control scheme in mixed product process, we conduct other mixed product controllers, t-EWMA [14], t-PCC [15] and JADE [13]. The overlay historical data include one tool, one product and two layers' input and output information (namely P1 and P2). The overlay process tool, Canon AFP 6000 ES6 scanner, was provided by Powerchip Technology Corporation (PSC). The overlay process model can be represented as:

$$\mathbf{y}_{i,k} = \boldsymbol{\alpha}_i + \boldsymbol{\beta}_i \mathbf{u}_{i,k} + \boldsymbol{\delta}_{i,k} \quad i = 1, 2 \tag{16}$$

where $\mathbf{y}_{i,k}$ denotes output parameters of product i, $\mathbf{y} = [\text{A1, A2, A3, A4, A5, B5, X7, X8, Y7, Y8}]^{\text{T}}$, $\mathbf{u}_{i,k}$ denotes recipe of product i, $\mathbf{u} = [\text{A1, A2, A3, A4, A5, B5, X7, X8, Y7, Y8}]^{\text{T}}$, $\boldsymbol{\beta}_i$ denotes process gain of product i, $\boldsymbol{\beta} = diag\,[1, 1, 1, 1, 1, 1, 1, 1, 1, 1]$, $\boldsymbol{\alpha}_i$ denotes intercept of product i, and $\boldsymbol{\delta}_{i,k}$ denotes process disturbance of product i. The initial values of these four mixed product control scheme are obtained from historical data as shown in Table Ⅰ-Table Ⅲ. The model gain of control model is set the same as process gain, i.e., $\mathbf{b}_i = diag\,[1, 1, 1, 1, 1, 1, 1, 1, 1, 1]$. The historical overlay data used in the simulation had been processed by the moving average 3 (MA(3)) controller, and the scheme of MA(3) for each overlay parameters is shown as follows:

$$u_{k+1} = T - \frac{\delta_k + \delta_{k-1} + \delta_{k-2}}{3} \tag{17}$$

where T denotes the target of these ten overlay output parameters, $T = 0$, the disturbance $\delta_k = y_k - u_k$ (namely "baseline" in PSC lithography overlay department) has also been used as a process disturbance for all controllers in this simulation.

TABLE I. INITIAL VALUES OF T-EWMA, T-PCC AND M-DEWMA CONTROL SCHEMES FOR P1

P1	*parameters*	*A1*	*A2*	*A3*	*A4*	*A5*
t-EWMA	$\hat{d}_{1,0}$	-0.0295	0.0379	0.0405	-0.0408	-0.0126
t-PCC	$\hat{d}_{1,0}$	-0.0295	0.0379	0.0405	-0.0408	-0.0126
	$\hat{p}_{1,0}$	0	0	0	0	0
m-dEWMA	$\hat{d}_{1,0}$	-0.0295	0.0379	0.0405	-0.0408	-0.0126
	$\hat{p}_0$	1.0E-5	-8.0E-6	6.0E-6	2.0E-6	2.0E-5
P1	***parameters***	***B5***	***X7***	***X8***	***Y7***	***Y8***
t-EWMA	$\hat{d}_{1,0}$	-0.0134	-3.4851	0.73005	0.9927	1.4119
t-PCC	$\hat{d}_{1,0}$	-0.0134	-3.4851	0.73005	0.9927	1.4119
	$\hat{p}_{1,0}$	0	0	0	0	0
m-dEWMA	$\hat{d}_{1,0}$	-0.0134	-3.4851	0.73005	0.9927	1.4119
	$\hat{p}_0$	3.0E-6	-0.0003	0.0005	-0.0004	0.0002

TABLE II. INITIAL VALUES OF T-EWMA, T-PCC AND M-DEWMA CONTROL SCHEMES FOR P2

P2	*parameters*	*A1*	*A2*	*A3*	*A4*	*A5*
t-EWMA	$\hat{d}_{2,0}$	-0.017	0.0315	0.01895	-0.0405	-0.0120
t-PCC	$\hat{d}_{2,0}$	-0.017	0.0315	0.01895	-0.0405	-0.0120
	$\hat{p}_{2,0}$	0	0	0	0	0
m-dEWMA	$\hat{d}_{2,0}$	-0.017	0.0315	0.01895	-0.0405	-0.0120
	$\hat{p}_0$	1.0E-5	-8.0E-6	6.0E-6	2.0E-6	2.0E-5
P2	***parameters***	***B5***	***X7***	***X8***	***Y7***	***Y8***
t-EWMA	$\hat{d}_{2,0}$	-0.0334	-4.1900	1.23614	-0.4086	1.8009
t-PCC	$\hat{d}_{2,0}$	-0.0334	-4.1900	1.23614	-0.4086	1.8009
	$\hat{p}_{2,0}$	0	0	0	0	0
m-dEWMA	$\hat{d}_{2,0}$	-0.0334	-4.1900	1.23614	-0.4086	1.8009
	$\hat{p}_0$	3.0E-6	-0.0003	0.0005	-0.0004	0.0002

TABLE III. THE INITIAL VALUES OF JADE CONTROL SCHEME

parameters	***A1***	***A2***	***A3***	***A4***	***A5***
$\hat{d}_{1,0}$ **(tool)**	-0.01291	0.020838	0.023694	-0.02321	-0.00282
$\hat{d}_{2,0}$ **(P1)**	-0.00624	0.008271	0.025439	-0.00847	-0.00333
$\hat{d}_{3,0}$ **(P2)**	-0.00667	0.012567	-0.00174	-0.01474	0.000506
parameters	***B5***	***X7***	***X8***	***Y7***	***Y8***
$\hat{d}_{1,0}$ **(tool)**	-0.00633	-2.40178	0.725731	0.13585	1.056041
$\hat{d}_{2,0}$ **(P1)**	-0.00191	-1.72257	0.644809	-0.33758	0.957915
$\hat{d}_{3,0}$ **(P2)**	-0.00442	-0.67922	0.080921	0.473428	0.098126

Table Ⅳ-Table Ⅴ list the weights of these four control schemes. The weights of these four control schemes are acquired by sweep method, which minimizes RMSE of the historical output data.

TABLE IV. THE OPTIMAL WEIGHTS SETTING FOR P1 IN SIMULATION

Weights		***A1***	***A2***	***A3***	***A4***	***A5***
t-EWMA		0.2	0.17	0.06	0.04	0.14
t-PCC	λ_1	0.18	0.17	0.05	0.03	0.12
	λ_2	0.01	0.01	0.01	0.01	0.01
JADE		0.08	0.05	0.03	0.02	0.06
m-dEWMA	$\lambda_{1,1}$	0.14	0.17	0.03	0.04	0.14
	λ_2	0.0001				
Weights		***B5***	***X7***	***X8***	***Y7***	***Y8***
t-EWMA		0.07	0.07	0.24	0.39	0.27
t-PCC	λ_1	0.03	0.06	0.23	0.38	0.26
	λ_2	0.01	0.01	0.01	0.01	0.01
JADE		0.03	0.06	0.06	0.12	0.05
m-dEWMA	$\lambda_{1,1}$	0.07	0.06	0.19	0.37	0.21
	λ_2	0.0001				

TABLE V. THE OPTIMAL WEIGHTS SETTING FOR P2 IN SIMULATION

Weights		***A1***	***A2***	***A3***	***A4***	***A5***
t-EWMA		0.12	0.08	0.06	0.05	0.14
t-PCC	λ_1	0.09	0.12	0.05	0.02	0.07
	λ_2	0.01	0.01	0.01	0.01	0.01
JADE		0.08	0.05	0.03	0.02	0.06
m-dEWMA	$\lambda_{1,2}$	0.11	0.13	0.07	0.04	0.08
	λ_2	0.0001				
Weights		***B5***	***X7***	***X8***	***Y7***	***Y8***
t-EWMA		0.06	0.17	0.06	0.26	0.01
t-PCC	λ_1	0.08	0.17	0.07	0.28	0.1
	λ_2	0.01	0.01	0.01	0.01	0.01
JADE		0.03	0.06	0.06	0.12	0.05
m-dEWMA	$\lambda_{1,2}$	0.09	0.18	0.09	0.29	0.12
	λ_2	0.0001				

The simulation results are shown in Table Ⅵ-Table Ⅸ and Figs. 3-8. Table Ⅵ shows the output RMSE values of these four mixed product controllers, and Table Ⅷ -Table Ⅸ demonstrate the improvement of these four mixed product controllers over the MA(3) controller. The bar chart of the ten output parameters for P1 and P2 addresses in Figs. 3-8. Based on the simulation results, the control performance of t-EWMA, t-PCC and m-dEWMA are similar in P1 and P2. However, the JADE control scheme presents deteriorated results in field term (X7, X8, Y7 and Y8 parameters) than the other three mixed product control schemes. Fig. 9 shows the historical data of A1 parameter for P1(abbreviated by P1 A1) which includes disturbance, input and output. It is observed that three outlier points exist in the disturbance trend nearby run 780^{th} marked by red circle in Fig. 9. Compared with the other input values nearby the outlier points, the input values of outlier points are abnormally higher than other ones. However, the output responses of outlier points exhibit normal behavior compared with other output values. Furthermore, it also shows that the input values of these outlier points do not follow the MA(3) controller, i.e., the outlier points are corresponding to the rework products. The abnormal disturbances caused by the rework products are the main reason why the control performance (RMSE) of these four mixed product control schemes is worse than that of the MA(3) controller.

Furthermore, due to tool-induced small drifting in overlay process, the compensation scheme of m-dEWMA does not reveal outstandingly control performance improvement over other three control schemes. In general, the simulation results reveal that the mixed product overlay process can be still improved by m-dEWMA control scheme even though the overlay process had been controlled by MA(3) controller.

TABLE VI. THE OUTPUT RMSE OF THESE FOUR MIXED PRODUCT CONTROL SCHEMES OF P1

P1 RMSE	***A1***	***A2***	***A3***	***A4***	***A5***
t-EWMA	0.00540	0.00332	0.01855	0.01781	0.01805
t-PCC	0.00542	0.00333	0.01838	0.01784	0.01813
JADE	0.00557	0.00368	0.01790	0.01850	0.01817
m-dEWMA	0.00545	0.00342	0.01898	0.01778	0.01808
MA(3)	0.00430	0.00368	0.02054	0.02112	0.02028
P1 RMSE	***B5***	***X7***	***Y7***	***X8***	***Y8***
t-EWMA	0.01740	0.43971	0.19170	0.21600	0.15299
t-PCC	0.01807	0.44144	0.19212	0.21670	0.15368
JADE	0.01673	0.46275	0.30103	0.26573	0.24143
m-dEWMA	0.01734	0.44222	0.19208	0.21732	0.15120
MA(3)	0.01897	0.37661	0.19231	0.26126	0.16836

TABLE VII. THE OUTPUT RMSE OF THESE FOUR MIXED PRODUCT CONTROL SCHEMES OF P2

P2 RMSE	*A1*	*A2*	*A3*	*A4*	*A5*
t-EWMA	0.00236	0.00240	0.010378	0.01283	0.010977
t-PCC	0.00237	0.00242	0.010413	0.01285	0.010937
JADE	0.00245	0.00257	0.010929	0.01302	0.011040
m-dEWMA	0.00236	0.00242	0.010372	0.01282	0.010907
MA(3)	0.00234	0.00245	0.011654	0.01360	0.012498
P2 RMSE	***B5***	***X7***	***Y7***	***X8***	***Y8***
t-EWMA	0.01009	0.27244	0.193193	0.17327	0.107557
t-PCC	0.01014	0.27351	0.194076	0.17395	0.10789
JADE	0.01007	0.28515	0.227805	0.18743	0.146669
m-dEWMA	0.01010	0.27245	0.193275	0.17364	0.10759
MA(3)	0.01128	0.29253	0.223569	0.17353	0.094182

TABLE VIII. THE IMPROVEMENT OF THESE FOUR CONTROL SCHEMES OVER MA3 CONTROLLER FOR P1

RMSE P1	*A1*	*A2*	*A3*	*A4*	*A5*
t-EWMA	-25.56%	9.84%	9.70%	15.67%	10.98%
t-PCC	-26.06%	9.47%	10.53%	15.53%	10.62%
JADE	-29.49%	-0.03%	12.84%	12.39%	10.38%
m-dEWMA	-26.81%	7.04%	7.58%	15.78%	10.83%
MA(3)					
RMSE P1	***B5***	***X7***	***Y7***	***X8***	***Y8***
t-EWMA	8.25%	-16.76%	0.31%	17.32%	9.13%
t-PCC	4.72%	-17.22%	0.09%	17.05%	8.72%
JADE	11.78%	-22.87%	-56.53%	-1.71%	-43.40%
m-dEWMA	8.60%	-17.42%	0.12%	16.82%	10.19%
MA(3)					

TABLE IX. THE IMPROVEMENT OF THESE FOUR CONTROL SCHEMES OVER MA(3) CONTROLLER FOR P2

RMSE P2	*A1*	*A2*	*A3*	*A4*	*A5*
t-EWMA	-0.87%	1.85%	10.95%	5.67%	12.17%
t-PCC	-1.13%	1.09%	10.65%	5.48%	12.49%
JADE	-4.46%	-4.97%	6.22%	4.25%	11.67%
m-dEWMA	-0.82%	1.16%	11.01%	5.71%	12.74%

MA(3)					
RMSE P2	***B5***	***X7***	***Y7***	***X8***	***Y8***
t-EWMA	10.60%	6.87%	13.59%	0.15%	-14.20%
t-PCC	10.13%	6.50%	13.19%	-0.24%	-14.55%
JADE	10.76%	2.52%	-1.89%	-8.01%	-55.73%
m-dEWMA	10.46%	6.86%	13.55%	-0.07%	-14.24%
MA(3)					

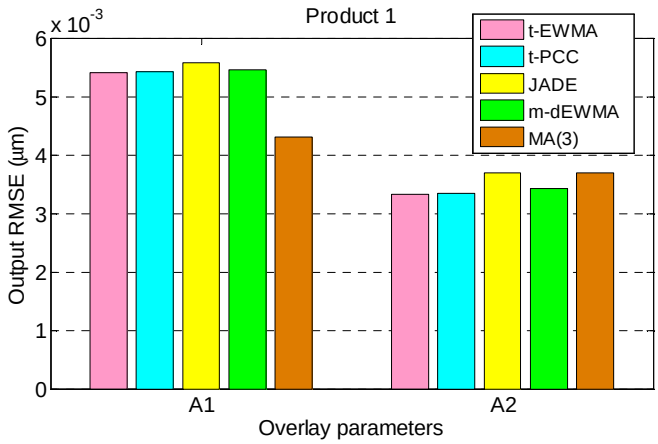

Figure 3. The output RMSE of A1 and A2 overlay parameters for P1

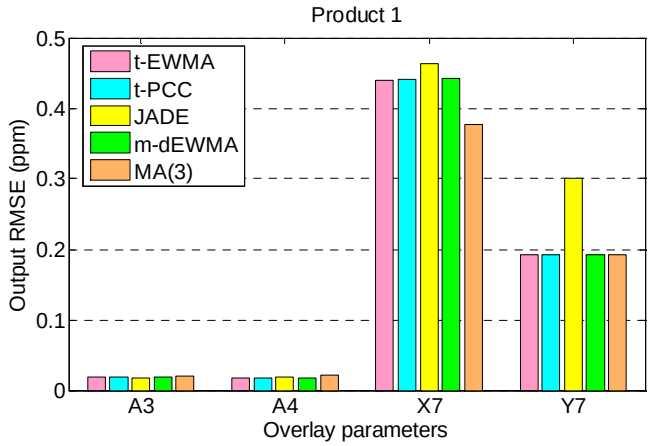

Figure 4. The output RMSE of A3, A4, X7 and Y7 overlay parameters for P1

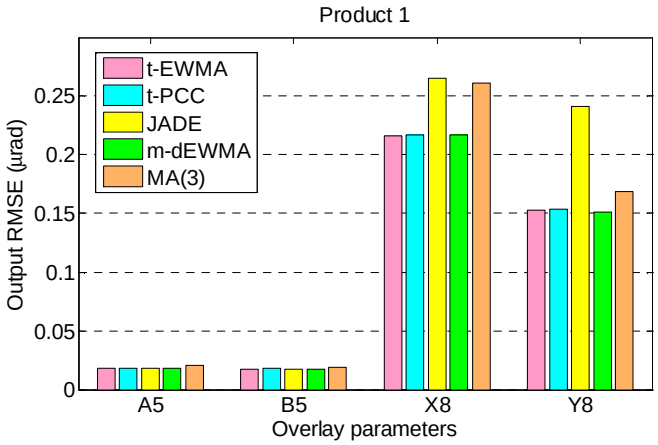

Figure 5. The output RMSE of A5, B5, X8 and Y8 overlay parameters for P1

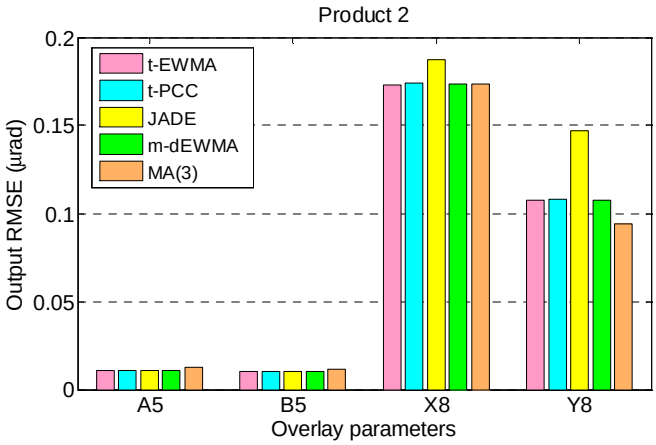

Figure 8. The output RMSE of A5, B5, X8 and Y8 overlay parameters for P2

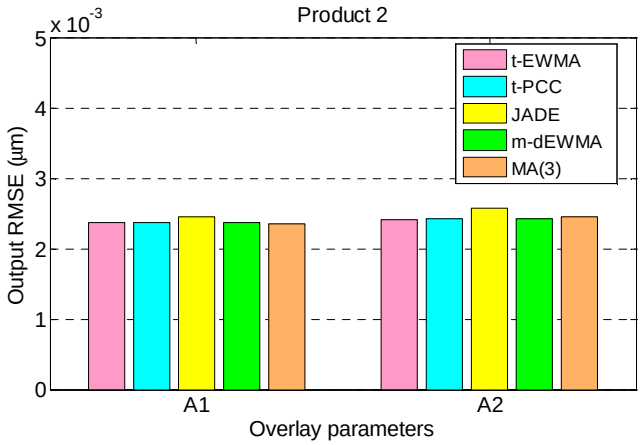

Figure 6. The output RMSE of A1 and A2 overlay parameters for P2

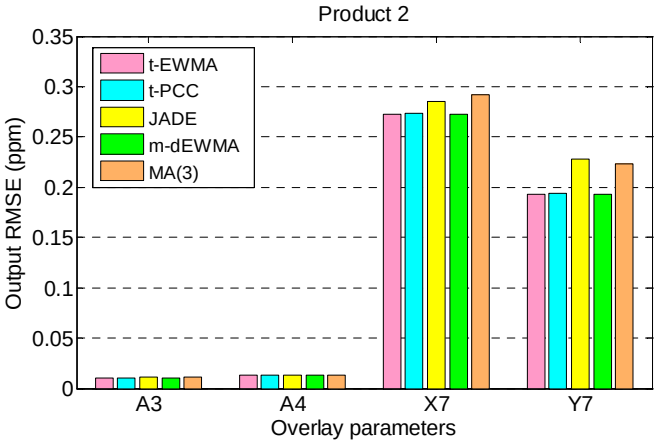

Figure 7. The output RMSE of A3, A4, X7 and Y7 overlay parameters for P2

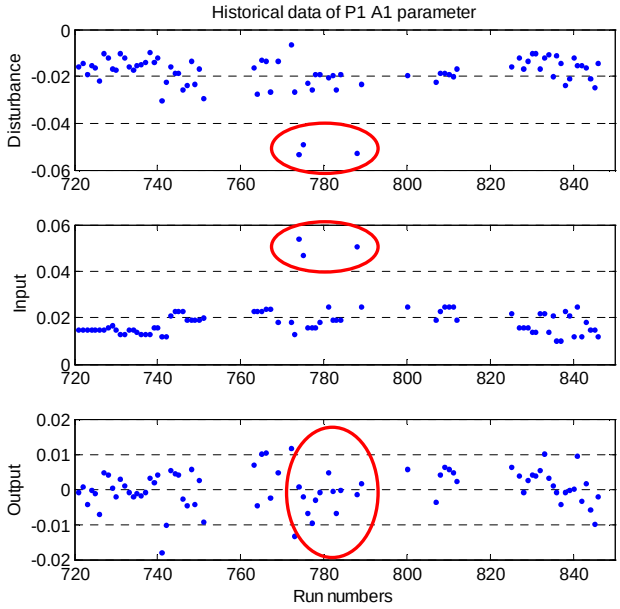

Figure 9. The historical data of P1 A1 parameter

IV. CONCULSION

This paper compares four RtR mixed product control schemes: t-EWMA, t-PCC, JADE and m-dEWMA, with actual overlay historical mixed product processes data, along with MA(3) method commonly used in semiconductor factories. The simulation results revealed that the control performance of t-EWMA, t-PCC and m-dEWMA are similar in Product 1 and Product 2 due to the tool-induced small drifting in historical overlay process data. Moreover, the control performance of t-EWMA, t-PCC and m-dEWMA have great resemblance to MA(3) method, i.e., these three mixed product control method could be used in actual overlay mixed product process. However, the JADE control scheme presents deteriorated results in field term (X7, X8, Y7 and Y8 parameters) than the other three mixed product control schemes.

ACKNOWLEDGMENT

The authors would like to thank the National Science Council of the Republic of China for financially supporting this paper under Contract NSC 100-2221-E-009-063-MY2.

REFERENCES

[1] M. A. Drew, M. G. Hanssmann, and D. Camporese, "Automation and Control for 300 mm Process Tools," Solid State Technol. vol. 40, no. 1, pp. 51-64, 1997.

[2] A. V. Prabhu and T. F. Edgar, "A new state estimation method for high-mix semiconductor manufacturing process," J. Process Control, vol. 19, no. 7, pp. 1149-1161, 2009.

[3] S. Adivikolanu and E. Zafiriou, "Extensions and Performance/Robustness Tradeoffs of the EWMA Run-to-Run Controller by Using the Internal Model Control Structure," IEEE Trans. Electron. Packag. Manuf., vol. 23, no. 1, pp. 56-68, January. 2000.

[4] E. D. Castillo, "Some Properties of EWMA Feedback Quality Adjustment Schemes for Drifting Disturbances," J. Qual. Technol., vol. 33, no. 2, pp. 153-166, April 2001.

[5] Z. C. Lin and W. J. Wu, "Multiple Linear Regression Analysis of the Overlay Accuracy Model," IEEE Trans. Semicond. Manuf., vol. 12, no. 2, pp. 229-237, May 1999.

[6] V. M. Martinez, K. Finn and T. F. Edgar, "Adaptive on-line estimation and control of overlay tool bias," Proc. SPIE, Advanced Process Control and Automation vol. 5044, pp. 52-62, 2003.

[7] C. A. Bode, B. S. Ko, and T. F. Edgar, "Run-to-run control and performance monitoring of overlay in semiconductor manufacturing," Control Engineering Practice, vol. 12, no. 7, pp. 893-900, 2004.

[8] S. A. Middlebrooks, "Optimal Model-Predictive Control of Overlay lithography implemented in an ASIC fab," SPIE, Advanced Process Control and Automation, vol. 5044, pp. 12–23, 2003.

[9] A. C. Lee, Y. R. Pan and M. T. Hsieh, "Output Disturbance Observer Structure Applied to Run-to-Run Control for Semiconductor Manufacturing." IEEE Trans. Semicond. Manuf., vol. 24, no. 1, pp. 27-43, February 2011.

[10] D. S. Lee and A. C. Lee, "Pheromone Propagation Controller: the Linkage of Swarm Intelligence and Advanced Process Control" IEEE Trans. Semicond. Manuf., vol. 22, no. 3, pp. 357-372, August 2009.

[11] J. H. Chen, T. W. Kuo and A. C. Lee, "Run-by-Run Process Control of Metal Sputter Deposition: Combining Time Series and Extended Kalman Filter," IEEE trans. Semicond. Manuf., vol. 20, no. 3, pp. 278-285, August 2007.

[12] C. F. Wu, C. M. Hung, J. H. Chen and A. C. Lee, "Advanced Process Control of the Critical Dimension in Photolithography," Int. J. of Precision Engineering and Manufacturing, vol. 9, no. 1, pp. 12-18, 2008.

[13] S. K. Firth, W. J. Campbell and A. Toprac, "Just-in-Time Adaptive Disturbance Estimation for Run-to-Run Control of Semiconductor Processes," IEEE Trans. Semicond. Manuf., vol. 19, no. 3, pp. 298-315, 2006.

[14] Y. Zheng, Q. H. Lin, D. S. H. Wang, S. S. Jang, and K. Hui, "Stability and performance analysis of mix product run-to-run control," J. Process Control, vol. 16, pp. 431-443, 2006.

[15] B. Ai, Y. Zheng, S. S. Jang, Y. Wang, L. Ye and C. Zhou, "The optimal drift-compensatory and fault tolerant approach for mixed-product run-to-run control," J. Process Control, vol. 19, no. 8, pp. 1401-1412, 2009

[16] B. Ai, Y. Zheng, Y. Wang, S. S. Jang and T. Song, "Cycle forecasting EWMA (CF-EWMA) approach for drift and fault in mixed-product run-to-run process," J. Process Control, vol. 20, no. 5, pp. 689-708, 2010.

[17] A. C. Lee, T. W. Kuo and Z. L. Lee, "Modified Double EWMA Approach for Mixed Product Run-to-Run CMP Process Control," Advanced Materials Research, vol. 314-316, pp. 2504-2511, August 2011.

[18] D. Schmidt and G. Charache, "Wafer process-induced distortion study for X-ray technology," J. Vac. Sci. Technol. B, vol. 9, no. 6, pp. 3237-3240, 1991

[19] M. A. Brink, C. G. M. Mol and R. A. George, "Matching performance for multiple wafer steppers using a advanced metrology procedure," Proc. SPIE: Integrated Circuit Metrology, Inspection, and Process Control Ⅱ, vol. 921, pp. 180-197, 1988.

[20] W. H. Arnold, "Image placement differences between 1:1 projection aligners and 10:1 reduction wafer steppers," Proc. SPIE: Optical Microlithography, vol. 394, pp. 87-98, 1983.